

COMPARISON OF SURFACE TOPOGRAPHY AFTER LENS-SHAPE END MILL AND BALL ENDMILL MACHINING

Porównanie topografii powierzchni po obróbce frezem soczewkowym oraz kulistym

Piotr ŻUREK ORCID 0000-0002-8735-6426
Karol ŻURAWSKI ORCID 0000-0002-7898-2628
Artur SZAJNA ORCID 0000-0002-3820-7272
Rafał FLEJSZAR ORCID 0000-0001-5231-6494
Marcin SAŁATA ORCID 0000-0002-2338-4380

DOI: 10.15199/160.2021.4.2

Abstract: The article presents the results of comparative investigations concerning surface topography obtained as a result of machining the workpiece with ball end and lens-shape end mills. The analysis was conducted for various values of width of cutting a_e and feed speed f_z . The research results include the comparison of surface topography maps and parameters of linear and surface roughness. It was shown, as a result of the research, that the use of lens-shape end mill allows to obtain similar values of surface topography parameters to the obtained values in machining with ball end mill, while achieving more than twice the efficiency of machining. As a result, there was demonstrated the potential for the use of lens-shape end mills in finishing operations as a useful alternative to ball end mills.

Keywords: lens-shape end mill, barrel end mill, ball end mill, surface topography, surface roughness

Streszczenie: W artykule przedstawiono wyniki badań porównawczych topografii powierzchni uzyskanych po obróbce przedmiotu frezem kulistym oraz soczewkowym. Analizę przeprowadzono dla różnych wartości szerokości skrawania a_e oraz prędkości posuwu f_z . Wyniki badań obejmują porównanie map topografii powierzchni oraz parametrów chropowatości liniowych i powierzchniowych. W wyniku badań wykazano, że zastosowanie freza soczewkowego pozwala na uzyskanie zbliżonych wartości parametrów topografii powierzchni jak po obróbce frezem kulistym, osiągając przy tym ponad dwa razy większą wydajność obróbki. W rezultacie wykazano potencjał zastosowania frezów soczewkowych w operacjach wykończeniowych jako użytecznej alternatywy dla narzędzi kulistych.

Słowa kluczowe: frez soczewkowy, frez baryłkowy, frez kulisty, topografia powierzchni, chropowatość powierzchni

Introduction

Currently, the five-axis milling method is widely used in the production of components with complex geometry in many branches of industry. Thanks to its flexibility, this technology found its success in the production of parts for several industries like aviation, automotive, tool, energy and medical industries. Additionally, five-axis milling is subject to increasing expectations both in terms of dimensional accuracy and surface quality of manufactured products.

In the case of finishing machining freeform surfaces, the types of mills with the widest use are the ball end mills (Fig. 1a). Their main advantage is a wide range of applicability in relation to the shape of the machined surface and easy generation of tool paths. However, the machining process using ball end mills shows a very low efficiency due to the large quantity of tool paths required [4–7].

The popularity of ball end mills is reflected in a very large number of scientific studies. The issues related to the mechanics and dynamics of the process were taken

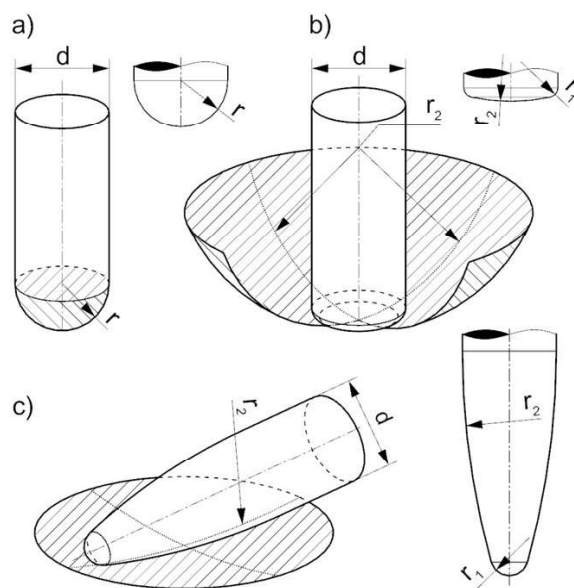


Fig. 1. Diagram of: a) ball end mill ($d = 2 \cdot r$). b) lens-shape end mill ($d \ll 2 \cdot r_2$). c) oval-form end mill ($d \ll 2 \cdot r_2$)

up by Altinas et al. [1, 8]. In their work, they developed a mathematical description of the geometry of the ball end milling cutter and model of the cutting layer cross-section as well as proposed mechanistic equations for the components of the cutting force.

Larue, Ferry et al. [9, 10, 12] extended the analysis with the peripheral milling. Moreover, Wojciechowski [22] proposed a model of the components of the cutting force, vibration, deformation and tool wear when machining hardened steels. Additionally, Ghorbani et al. [11] included the values of the principal curvatures of the machined freeform surface and the values of the radial runout of the mill in the cutting force model.

The subject of surface topography obtained after machining with a ball end mill was discussed by Arizmendi et al. [2]. They proposed an analytical model for determining the surface topography after machining with a ball end mill based on the trajectory of the cutting edge movement, taking into account technological parameters such as tool feed, cutting depth, cutting width and tool radial runout. Moreover, Seyed Ehsan et al. [15] continued the issue for the case of five-axis machining. They proposed a method for determining the surface topography in which the position of the tool axis was taken into account by defining the lead and tilt angles.

Due to the intensive development of CAM software, it is becoming more frequent to use the tools with unusual shapes. Circle segment end mills are gaining more and more popularity, especially in the finishing of freeform surfaces. The geometry of these tools is defined by an arc, whose radius r_2 is many times greater than the radius of the tool shank $d/2$ [24, 25]. This solution makes possible maintaining the desired surface quality, while significantly reducing the number of tool paths. However, the main disadvantage of that type of tools is the limited positioning range in relation to the machined surface [4–7].

Scientific studies concerning the circle segment end mills most often put their focus on barrel-shape and oval form tools. Artxe, Urbikain et al. [3] presented a mathematical description of the geometry of an oval form endmill and proposed a mechanistic model of cutting force components with reference to the radial runout of the tool. In subsequent works [16, 17, 19] the model was developed further by analysing the influence of the lead angle, tilt angle and vibrations on the distribution of cutting force components. This issue was also developed for barrel-shape tools in the work of Olver et al. [14].

Urbikan et al. [18, 20] presented a mathematical and empirical models for the determination of surface roughness after machining with an oval form and a barrel-shape mill. The issues of positioning and generating a tool path of the barrel-shape end mills were taken up in the work of Wang et al. [21], YaoAn et al. [23] and Ming et al. [13]. Each of the works presents different algorithms for determining the position of the tool axis and points of contact with the machined surface in the case of peripheral milling.

One type of circle-segment end tools is the lens-shape end mill. Despite the availability of the solution of this type of mills offered by tool manufacturers, there is no scientific literature on this subject. The aim of this study is to demonstrate the applicability of lens-shape end mills as an alternative to ball end mills in five-axis finishing milling operations.

Materials and methods

The first stage of the research was to perform a finishing operation of the test workpiece, consisting of a surface divided into 16 areas (Fig. 3). Different values of the path width b_f and the tool feedrate v_f were used for each of 16 machined areas. Tests numbered 1 – 8 were carried out with a EMUGE FRANKEN 3544L.10020A lens-shape end mill with a radius of $r_2 = 40$ [mm] (Fig. 2a), while tests numbered 9 – 16 were performed using a Sandvik Coromant R216.42-10030-AC19P 1620 ball end mill with a radius $r = 5$ [mm] (Fig. 2b). Both tools were mounted in a Sandvik Coromant 930-HA06-HD-20-104 holder with the same overhang equal to 37 [mm].

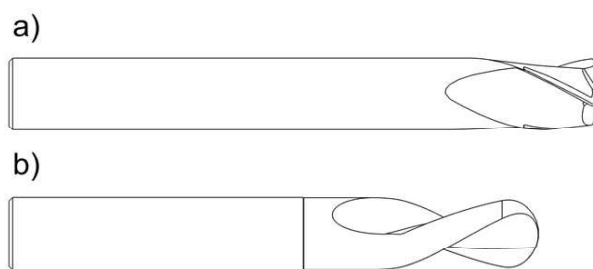


Fig. 2. Tools used for tests a) lens-shape end mill EMUGE FRANKEN 3544L.10020A b) ball end mill Sandvik Coromant R216.42-10030-AC19P 1620

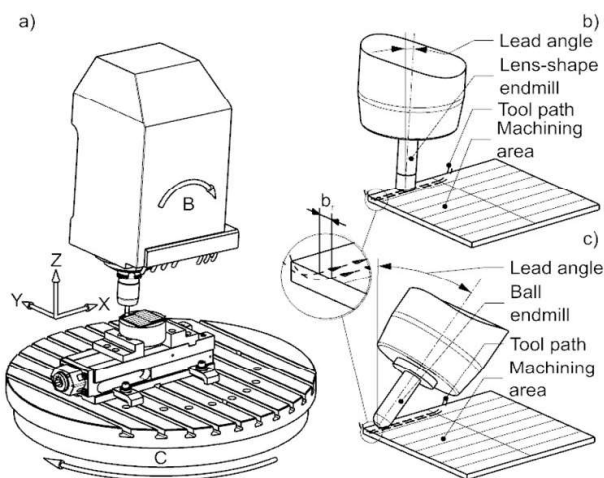


Fig. 3. Scheme of a) machine tool configuration, b) lens-shape end mill machining, c) ball end mill machining

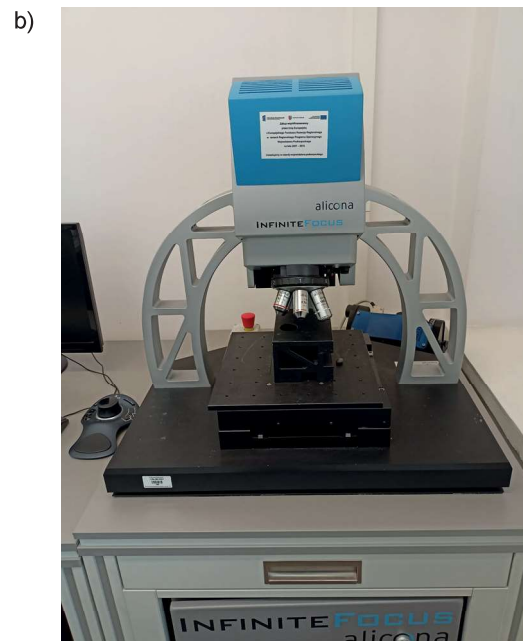


Fig. 4. Research—measurement stand: a) DMU 100 monoBLOCK milling centre. b) 3Dsystem InfiniteFocus Alicona optical microscope

In each operation, a lead angle was used to avoid contact of the tool tip with the machined surface, which would result in a machining at zero cutting speed. In the case of the lens-shape end mill, the lead angle was set to 4° (Fig. 3b). Using a larger value would engage the radius r_f in machining. On the other hand, for the ball end mill, a lead angle of 45° was set in order to achieve the maximum effective diameter of the tool (Fig. 3c). In this case, setting a larger lead angle would result in a collision

of the tool holder with the workpiece. The tests were carried out on a DMU 100 monoBLOCK multi-axis milling center (Fig. 4a). The material machined during the tests was 42CrMo4 steel. The technological and kinematic parameters used during machining are presented in table 1.

The next stage of the research was focused on measurements of the machined surface topography. They were performed using the 3Dsystem Infinite Focus Alicona optical microscope (Fig. 4b).

Table 1. Technological and kinematic parameters used during the first stage of the test

No	Tool	Cutting width b_p [mm]	Cutting depth a_p [mm]	Tool feed v_f [mm/min]	Spindle speed n [min ⁻¹]	Lead angle [°]	Tilt angle [°]
1	Lens-shape end mill Emuge Franken 3544L.10020A	0.2	0.2	1145.85	7939	4	0
2		0.4					
3		0.6					
4		0.8					
5		0.2		1604.19			
6		0.4					
7		0.6					
8		0.8					
9	Ball end mill Sandvik Coromant R216.42-10030-AC19P 1620	0.2		1145.85	7939	45	
10		0.4					
11		0.6					
12		0.8					
13		0.2		1604.19			
14		0.4					
15		0.6					
16		0.8					

Results and Discussion

For all measured surface roughness profiles, the values of the profile roughness parameters R_a , R_q , R_z , R_t (Fig. 5) show similar trends. As the path width increases

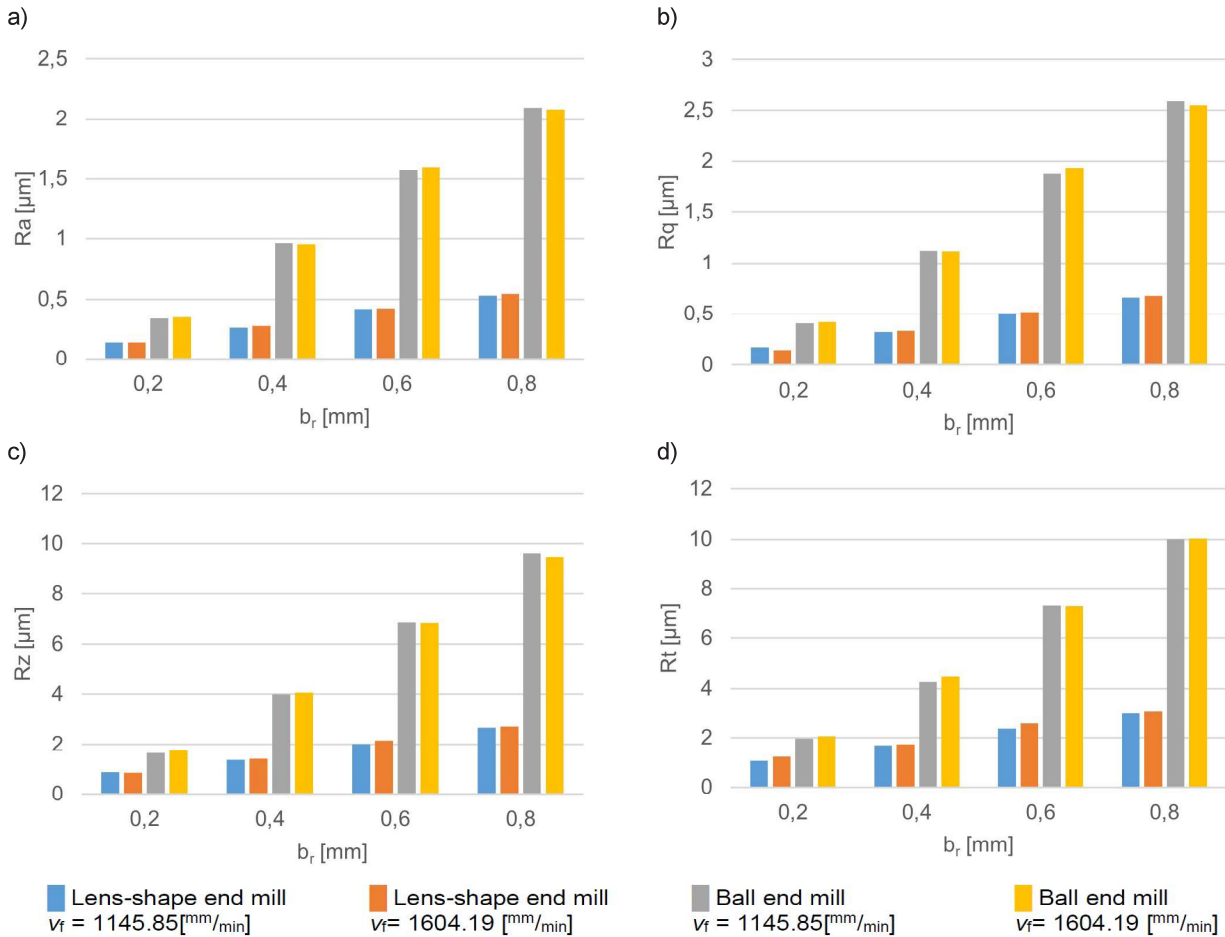


Fig. 5. Graphs depicting profile parameters of surface roughness a) arithmetic mean deviation – R_a . b) Root mean square deviation – R_q . c) Maximum height – R_z . d) Total height – R_t

In the case of machining with a ball end mill, along with the increase in the width of the tool path, the surface roughness value increases significantly. It is particularly noticeable in the case of low path widths – when changing the b_r from 0.2 [mm] to 0.4 [mm] an increase in all roughness parameters by over 100% is visible. With a further increase in the b_r parameter, the increase in the roughness parameters for the subsequent steps is approximately 50% and 30%, respectively.

Measurements of the roughness of the surface milled with a lens-shape end mill show lower values compared to the surface machined with a ball end mill. For the path width $b_r = 0.2$ [mm], it can be observed that the values of R_a and R_q parameters constitute 30% of the values obtained for the surface machined with a ball end mill, and for R_z and R_t they equate to 50% of this value. An increase in b_r parameter causes an increase in the roughness parameters. By analysing and comparing the values

linearly. The roughness parameters increase in an approximately linear manner. The change in tool feed did not significantly affect the results because the discrepancies it caused were within the measurement error margin.

of the roughness parameters, in particular for larger path widths, at least a 70% decrease in the roughness parameters values is visible.

All areal roughness parameters computed from measurement data show similar tendencies. As the path width b_r increases linearly, there is an approximately exponential increase in the surface stereometry parameters S_a , S_q , S_z , S_t (Fig. 6). This tendency is particularly visible on the measured surface topographies (Tab. 2), where the increase of the path width b_r is much more significant in the upper ranges of the b_r values. It is noteworthy, that for a lens-shape end mill the exponent is smaller than for a ball mill. This relationship is clearly visible on the measured topography which shows much greater differentiation for the ball mill. At higher b_r values, when comparing the analysed cutters, the results of measurements are characterized by much greater differences. For $v_f = 1604.19$ [mm/min] with $b_r = 0.2$ [mm] the

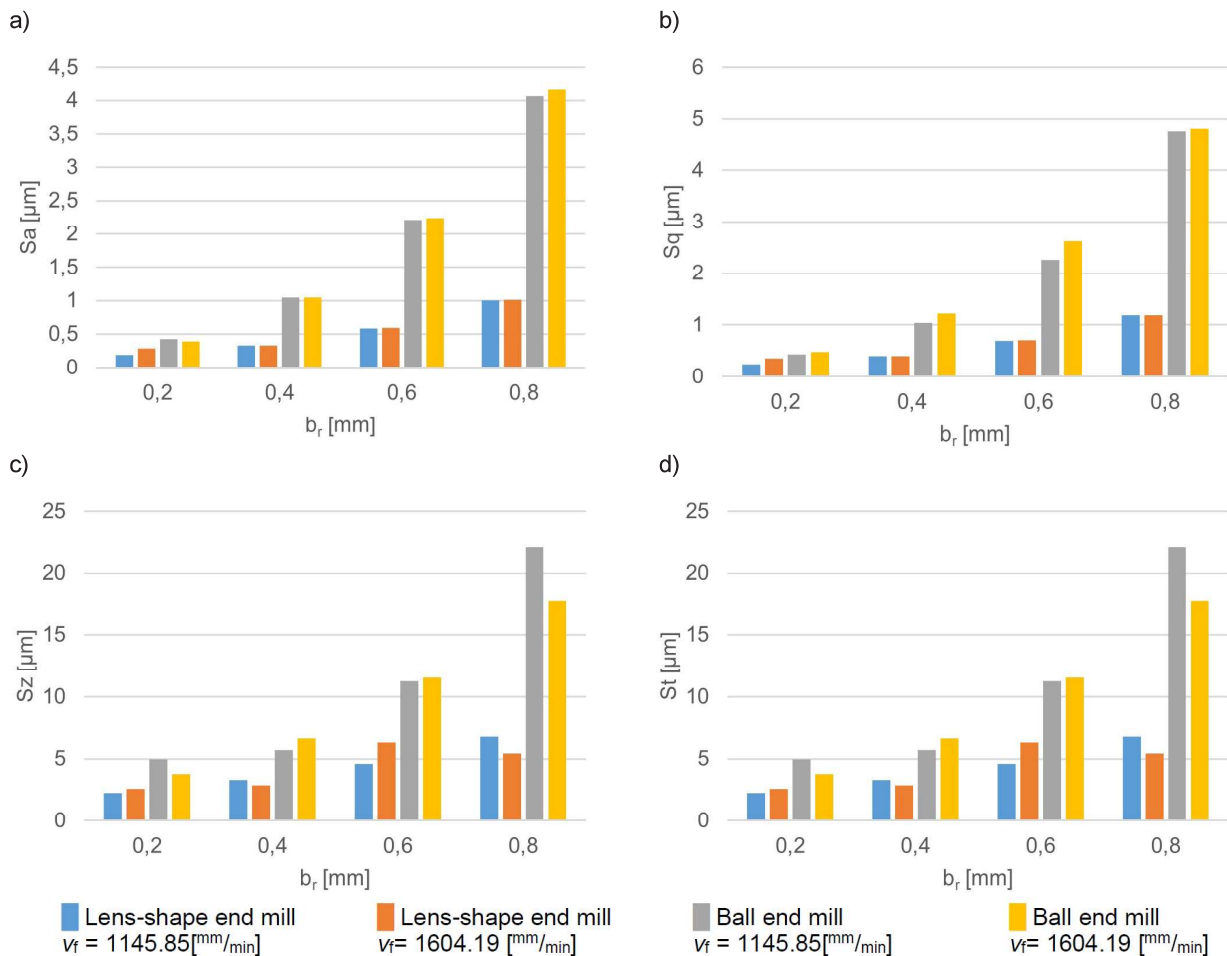



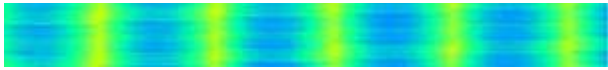







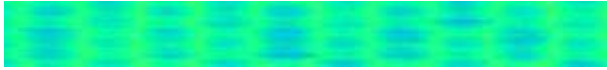



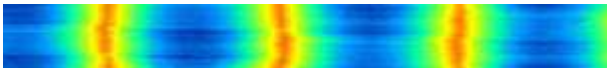


Fig. 6. Graphs depicting areal surface parameters of roughness a) arithmetic mean deviation – S_a . b) Root mean square deviation – S_q . c) Maximum height – S_z . d) Total height – S_t .

difference in the S_q parameters for both end mills is only about $0.2 \mu\text{m}$. After the increase to $b_r = 0.8 \text{ [mm]}$, the measurement of the S_q parameter of the surface machined by the lens-shape end mill was $1.1937 \mu\text{m}$, and for the ball end mill it was $4.8151 \mu\text{m}$. This means that for S_q parameter, using a lens-shape end mill with a large path width b_r , it was possible to achieve a 75% reduction of the measured value. In the case of areal surface

roughness parameters, similarly to the profile roughness parameters, no significant changes resulting from a change in tool feed were observed. The only inaccuracy is in the measurement of the parameter S_z and S_t , where for $b_r = 0.8 \text{ [mm]}$ there was observed a decrease in the value of the roughness parameter with increasing tool feed. It can probably be caused by external disturbances or vibrations in the cutting process.

Table 2. Surfaces topography after milling

<p>N° 1: $v_f = 1145.85 \text{ [mm/min]}$ $b_r = 0.2 \text{ [mm]}$ $S_a = 0.19470 \text{ [}\mu\text{m]}$ $S_q = 0.24274 \text{ [}\mu\text{m]}$</p> 	<p>N° 9: $v_f = 1145.85 \text{ [mm/min]}$ $b_r = 0.2 \text{ [mm]}$ $S_a = 0.42792 \text{ [}\mu\text{m]}$ $S_q = 0.52928 \text{ [}\mu\text{m]}$</p> 
<p>N° 2: $v_f = 1145.85 \text{ [mm/min]}$ $b_r = 0.4 \text{ [mm]}$ $S_a = 0.32818 \text{ [}\mu\text{m]}$ $S_q = 0.40083 \text{ [}\mu\text{m]}$</p> 	<p>N° 10: $v_f = 1145.85 \text{ [mm/min]}$ $b_r = 0.4 \text{ [mm]}$ $S_a = 1.0423 \text{ [}\mu\text{m]}$ $S_q = 1.2251 \text{ [}\mu\text{m]}$</p> 

<p>N° 3: $v_f = 1145.85$ [mm/min] $b_r = 0.6$ [mm] $Sa = 0.57917$ [μm] $Sq = 0.68962$ [μm]</p> 	<p>N° 11: $v_f = 1145.85$ [mm/min] $b_r = 0.6$ [mm] $Sa = 2.2159$ [μm] $Sq = 2.5983$ [μm]</p> 
<p>N° 4: $v_f = 1145.85$ [mm/min] $b_r = 0.8$ [mm] $Sa = 1.0025$ [μm] $Sq = 1.1867$ [μm]</p> 	<p>N° 12: $v_f = 1145.85$ [mm/min] $b_r = 0.8$ [mm] $Sa = 4.0601$ [μm] $Sq = 4.7517$ [μm]</p> 
<p>N° 5: $v_f = 1604.19$ [mm/min] $b_r = 0.2$ [mm] $Sa = 0.28247$ [μm] $Sq = 0.35433$</p> 	<p>N° 13: $v_f = 1604.19$ [mm/min] $b_r = 0.2$ [mm] $Sa = 0.39209$ [μm] $Sq = 0.47982$ [μm]</p> 
<p>N° 6: $v_f = 1604.19$ [mm/min] $b_r = 0.4$ [mm] $Sa = 0.33048$ [μm] $Sq = 0.40120$ [μm]</p> 	<p>N° 14: $v_f = 1604.19$ [mm/min] $b_r = 0.4$ [mm] $Sa = 1.0463$ [μm] $Sq = 1.2352$ [μm]</p> 
<p>N° 7: $v_f = 1604.19$ [mm/min] $b_r = 0.6$ [mm] $Sa = 0.58755$ [μm] $Sq = 0.70416$ [μm]</p> 	<p>N° 15: $v_f = 1604.19$ [mm/min] $b_r = 0.6$ [mm] $Sa = 2.2358$ [μm] $Sq = 2.6240$ [μm]</p> 
<p>N° 8: $v_f = 1604.19$ [mm/min] $b_r = 0.8$ [mm] $Sa = 1.0094$ [μm] $Sq = 1.1937$ [μm]</p> 	<p>N° 16: $v_f = 1604.19$ [mm/min] $b_r = 0.8$ [mm] $Sa = 4.1592$ [μm] $Sq = 4.8151$ [μm]</p> 

Conclusions

The results of research allow to draw the following conclusions:

- As the path width b_r increases, all the measured values of the surface geometrical structure parameters increase. However, the surface geometrical structure parameters increase with the path width b_r exponentially. At the same time the profile roughness parameters increase with the path width b_r linearly (fig. 5).
- The surfaces machined with a lens-shape mill is characterised by a lower roughness compared to the surfaces machined with ball end mill, especially when larger values of the path width b_r , even up to 75%, are considered.
- The feed in the range of values applied in the tests does not significantly affect the roughness parameters.

The research shows that the use of a lens-shape end mill allows for obtaining values of the surface topography parameters similaras the ones after the machining with a ball mill. with more than a double of the path width b_r ,

The potential of using lens-shape end mills in finishing operations as an alternative to ball mills provides grounds to continue research in the same direction as for other circle segment end mills.

References

- [1] Altintas. Y. Lee. P. 1998. "Mechanics and Dynamics of Ball End Milling." Journal of Manufacturing Science and Engineering. Transactions of the ASME 120 (4): 684–92.
- [2] Arizmendi. M. Fernández J., López de Lacalle L. N., Lamikiz A. Gil A. Sánchez J. A. Campa F. J. Veiga F. 2008. „Model development for the prediction of surface topography generated by ball-end mills taking into account the tool parallel axis offset. Experimental validation." CIRP Annals - Manufacturing Technology 57 (1): 101–104.
- [3] Artetxe. E. Urbikain G. Lamikiz A. López-De-Lacalle L. N., González R. Rodal P. 2015. "A mechanistic cutting force model for new barrel end mills". Procedia Engineering 132: 553–560.
- [4] Burek J. Żurek P. Żurawski K. Sułkiewicz P. 2016. "Programowanie procesu 5-osiowej symultanicznej

- obróbki frezem baryłkowym w aplikacji HyperMILL". *Mechanik* 2016/5-6: 470–471.
- [5] Burek J. Żurek P. Żurawski K. 2016. "Porównanie chropowości powierzchni złożonych po obróbce frezem baryłkowym oraz kulistym". *Mechanik* 2016/10: 1476–1477.
- [6] Burek J. Żyłka Ł. Żurek P. Żurawski K. Sałata M. 2017. "Badania symulacyjne warstwy skrawanej frezem baryłkowym". *Mechanik* 2017/8-9:714–716.
- [7] Burek J. Żurek P. Żurawski K. 2018 "Badania symulacyjne siły skrawania w procesie obróbki frezem baryłkowym". *Mechanik* 2018/10: 901–903.
- [8] Engin S. Altintas Y. 1999 „Generalized modeling of milling mechanics and dynamics: Part I - helical end mills.” American Society of Mechanical Engineers, Manufacturing Engineering Division 10: 345–352.
- [9] Ferry W.B.S. 2008 „Virtual five-axis flank milling of jet engine impellers.” The University Of British Columbia.
- [10] Ferry W.B. Altintas Y. 2008 „Virtual five-axis flank milling of jet engine impellers - Part I: Mechanics of five-axis flank milling.” *Journal of Manufacturing Science and Engineering*. Transactions of the ASME 130: 0110051–01100511.
- [11] Ghorbani, M., Movahhedy M. R. 2019. "Extraction of Surface Curvatures from Tool Path Data and Prediction of Cutting Forces in the Finish Milling of Sculptured Surfaces." *Journal of Manufacturing Processes* 45 (September): 273–89.
- [12] Larue, A. Altintas Y. 2005. „Simulation of Flank Milling Processes.” *International Journal of Machine Tools and Manufacture* 45 (4–5): 549–59.
- [13] Ming L. Dongqing Y. Baohai W. Dinghua Z. 2016. „Barrel cutter design and toolpath planning for high-efficiency machining of freeform surface”. *International Journal of Advanced Manufacturing Technology* 85 (9–12): 2495–2503. Olvera, D. E. Artetxe, M. Luo, and G. Urbikain. 2020. „5-axis milling of complex parts with barrel-shape cutter: cutting force model and experimental validation”. *Procedia Manufacturing* 48 (2019): 528–532.
- [14] Seyed Ehsan, L. K. Ismail L. 2017. „3D surface topography analysis in 5-axis ball-end milling”. *CIRP Annals - Manufacturing Technology* 66 (1): 133–136.
- [15] Urbikain, G. Olvera D. López de Lacalle L.N. 2016. „Stability Contour Maps with Barrel Cutters Considering the Tool Orientation.” *The International Journal of Advanced Manufacturing Technology* 2016 89:9 89 (9): 2491–2501.
- [16] Urbikain, G. Artetxe E. López de Lacalle L. N. 2017. „Numerical simulation of milling forces with barrel-shaped tools considering runout and tool inclination angles” *Applied Mathematical Modelling* 47: 619–636.
- [17] Urbikain, G. L. N. López de Lacalle. 2018. „Modelling of surface roughness in inclined milling operations with circle-segment end mills”. *Simulation Modelling Practice and Theory* 84: 161–176.
- [18] Urbikain Pelayo, G. 2019. "Modelling of static and dynamic milling forces in inclined operations with circle-segment end mills". *Precision Engineering* 56 (3): 123–135.
- [19] Urbikain Pelayo, G. Olvera-Trejo D. Luo M. López-De-Lacalle L. N. Elías-Zuniga A. 2021. „Surface roughness prediction with new barrel-shape mill considering runout: Modeling and validation”. *Measurement* 173: 1–10.
- [20] Wang, D. Wu Yi C. Tian L. Ru Feng X. 2009. „Five-axis flank milling of sculptured surface with barrel cutters”. *Key Engineering Materials* 407–408 (2): 292–297.
- [21] Wojciechowski S. 2014 „Siły w procesie skrawania frezem kulistym zahartowanej stali” *Politechnika Poznańska. Wydział Budowy Maszyn i Zarządzania*. Poznań.
- [22] YaoAn, L. QingZhen B. BaoRui D. ShuLin C. LiMin Z. Kai H. 2014. „Five-axis strip machining with barrel cutter based on tolerance constraint for sculptured surfaces” *International Journal of Mechanical Aerospace, Industrial Mechatronic and Manufacturing Engineering* 8 (10): 1779–1784.
- [23] EMUGE Corp. „Circle Segment Cutters.” <https://www.emuge.com/sites/default/files/literature/Circle-Segment-Turbine-Catalog-2020.pdf> (2021.07)
- [24] Hoffman Group. „Dynamic 5-axis milling with GARANT PPC mills and PPC indexable inserts.” <https://www.hoffmann-group.com/US/en/areas-of-application/machining/solid-carbide-barrel-milling-cutter-garant-ppc/e/68093/>. (2021.07).

mgr inż. Piotr Żurek

Rzeszów University of Technology, Faculty of Mechanical Engineering and Aeronautics, Department of Manufacturing Techniques and Automation
ul. Wincentego. Pola 2 35-959 Rzeszów, Poland
e-mail: p_zurek@prz.edu.pl

mgr inż. Karol Żurawski

Rzeszów University of Technology, Faculty of Mechanical Engineering and Aeronautics, Department of Manufacturing Techniques and Automation
ul. Wincentego. Pola 2 35-959 Rzeszów, Poland
e-mail: zurawski@prz.edu.pl

mgr inż. Artur Szajna

Rzeszów University of Technology, Faculty of Mechanical Engineering and Aeronautics, Department of Manufacturing Techniques and Automation
ul. Wincentego. Pola 2 35-959 Rzeszów, Poland
e-mail: a.szajna@prz.edu.pl

mgr inż. Rafał Flejszar

Rzeszów University of Technology, Faculty of Mechanical Engineering and Aeronautics, Department of Manufacturing Techniques and Automation
ul. Wincentego. Pola 2 35-959 Rzeszów, Poland
e-mail: r.flejszar@prz.edu.pl

mgr inż. Marcin Sałata

Rzeszów University of Technology, Faculty of Mechanical Engineering and Aeronautics, Department of Manufacturing Techniques and Automation
ul. Wincentego. Pola 2 35-959 Rzeszów, Poland
e-mail: msalata@prz.edu.pl



Like us on Facebook
www.facebook.com/sigmanot



Follow us on Instagram
www.instagram.com/sigmanot

WYDZIAŁ BUDOWY MASZYN I ZARZĄDZANIA